ELSEVIER

Journal of Molecular Catalysis A: Chemical 158 (2000) 199–208

JOURNAL OF MOLECULAR CATALYSIS A: CHEMICAL

www.elsevier.com/locate/molcata

Mechanistic insights in the activation of oxygen on oxide catalysts for the oxidative dehydrogenation of ethane from pulse experiments and contact potential difference measurements

E.V. Kondratenko [*,1], O. Buyevskaya, M. Baerns

Institute for Applied Chemistry Berlin-Adlershof, Richard-Willstätter-Str. 12, D-12484 Berlin, Germany

Dedicated to Professor Dr. Manfred Meisel on the occasion of his 60th birthday

Abstract

The oxidative dehydrogenation of ethane (ODE) was studied over Na_2O/CaO, Sm_2O_3/CaO and Sm_2O_3 catalysts at 923 K using different oxygen partial pressures. The type of interaction of oxygen with these catalysts was derived from measurements of contact potential difference (CPD) between a gold electrode and the catalysts and pulse experiments in the Temporal Analysis of Product (TAP) reactor. Modelling of TAP oxygen responses in the temperature range from 673 to 873 K showed that a reversible dissociative adsorption via a molecular precursor provides a good description of the measured transient responses for all catalysts. Supplementary CPD results confirmed the transformation of adsorbed molecular oxygen species to atomic ones. Rate constants and activation energies of the elementary reaction steps of oxygen adsorption, desorption, dissociation and association were estimated from the TAP oxygen responses. The dependence of ethylene selectivity both on doping and oxygen partial pressure was explained by the ratio of Θ_O/Θ_{O_2}. This ratio is strongly affected by the constants of adsorption of oxygen and dissociation of molecular adsorbed oxygen.

Keywords: Temporal of products (TAP) reactor; Contact potential difference; Modelling of oxygen adsorption; Oxidative dehydrogenation of ethane; Mixed oxide catalysts

1. Introduction

The interaction of gas-phase oxygen with oxide catalysts is an important step in the partial oxidation of hydrocarbons [1–3]. The reaction pathways are significantly influenced by the type of surface oxygen species formed via this interaction, which are involved in both reactant activation and secondary reactions. In most cases, the selective transformation of light paraffins to olefins and oxygenates does not occur with a reasonable selectivity since the desired products being intermediates in the overall process can be easily oxidised to CO_x. Indication that hydrocarbon oxidation is strongly related to the state of oxygen species results from earlier work of Iwamoto and Lunsford [4].

[*] Corresponding author. Tel.: +49-30-63924448; fax: +49-30-63924454.

E-mail address: evgenii@aca-berlin.de (E.V. Kondratenko).

[1] Permanent address: Institute of Chemistry and Chemical Technology, K. Marx Str. 42, 660049 Krasnoyarsk, Russia.

1381-1169/00/$ - see front matter
PII: S1381-1169(00)00066-2

They reported that multi-atomic oxygen species promote C–C bond cleavage, but monoatomic oxygen species do not promote this reaction. The present authors [5,6] drew a similar conclusion from measurements of total conductivity and contact potential difference (CPD) between a gold electrode and doped rare-earth oxides. The replacement of oxygen by nitrous oxide, as an oxidant, enhances also the selectivity of desired reaction products [7,8]. The increase of selectivity was explained by formation of only atomic oxygen species from N_2O. Thus, the regulation of oxygen activation may be one of the possibilities to control the selective oxidation.

For the oxidative dehydrogenation of ethane (ODE), mixed oxide systems consisting of rare-earth, alkali-earth and alkali oxides are known as catalysts [9–12]; high ethylene yields and selectivities in particular at $T > 550$°C were achieved. Morales and Lunsford [9] reported an ethylene selectivity of 74.8% ($X_{C_2H_6} = 39.3\%$) at 873 K using Li (3 wt.%)/MgO catalyst. A similar ethylene selectivity of 86.4% ($X_{C_2H_6} = 38\%$) was achieved by Swaan et al. [10] on Li/Na/MgO at 898 K. Lithium-doped lanthanum–calcium oxide (Li:La:Ca = 1:1:2.5) was described as an effective catalyst resulting in C_2H_4 yields of 48.2% ($S = 89.2\%$) at 893 K and GHSV = 1000 h^{-1} [11]. Ethylene yields of up to 34–45% ($S = 66$–73%) were obtained on REO-based catalysts (e.g. Na–P–Sm–O, Sm–Sr–O) under non-isothermal conditions ($T_{max} = 1083$–1138 K) at contact times in the order of 30 to 40 ms [12]. There is, however, only limited information regarding the key factors determining the catalytic activity and selectivity [9,12].

The aim of the present work is the elucidation of the oxygen interaction with Na_2O/CaO, Sm_2O_3/CaO and Sm_2O_3 catalysts using Temporal Analysis of Product (TAP) reactor and measurements of CPDs to further illustrate the dependence of catalyst selectivity on the type of surface oxygen. Kinetics and mechanistic insights obtained were used deriving a better understanding of the factors determining the selectivity in the ODE.

2. Experimental and methods

2.1. Catalysts

Na_2O/CaO catalysts were prepared from $CaCO_3$ (Alfa) and $NaHCO_3$ (Merck). $CaCO_3$ was calcinated at 1273 K for 10 h to decompose the carbonate. After calcination, the calcium oxide was impregnated with an aqueous solution of $NaHCO_3$ followed by drying at 400 K for 2 h and calcination at 1273 K for 2 h. After calcination, the actual sodium concentration was determined by inductively coupled plasma optical emission spectroscopy (ICP-OES). Catalysts of the following stoichiometry were prepared: $Na_{0,00001}CaO_x$, $Na_{0,009}CaO_x$, $Na_{0,012}CaO_x$ and $Na_{0,064}CaO_x$. The BET surface areas of the catalysts amounted to 6.3 m^2/g for $Na_{0,00001}CaO_x$, 2.3 m^2/g for $Na_{0,009}CaO_x$, 2.9 m^2/g for $Na_{0,012}CaO_x$ and 2 m^2/g for $Na_{0,064}CaO_x$.

Sm_2O_3 (Merck) was calcinated at 973 K for 4 h before TAP experiments; S_{BET} of the calcined product amounted to 5.6 m^2/g.

For preparation of a $SmCa_5O_x$ catalyst, a samarium nitrate solution was added to a suspension of $Ca(OH)_2$ in water. The mixture was stirred and heated to evaporate the water; the catalyst precursor was calcined at 700°C in a flow of air for 2 h; S_{BET} of the calcined catalyst amounted to 1.6 m^2/g.

2.2. Catalytic testing

The catalytic tests were performed in a fixed-bed reactor made of quartz. The feed gas consisted of 3–15 vol.% of oxygen and 30 vol.% of ethane in nitrogen. The total flow rate was fixed at 60 cm^3/min; the reaction temperature amounted to 923 K. For comparison of selectivities at similar degrees of hydrocarbons conversion, the tests were performed at different con-

tact times varying the amount of catalyst from 0.01 to 0.2 g. The feed gas and reaction products were analyzed on-line using a gas chromatograph (HP-5890) equipped with Poraplot Q and Molsiev 5 columns.

2.3. CPD measurements

The CPD between the samples and a reference gold electrode was measured by applying the vibrating condenser method. Details of the apparatus have been reported elsewhere [6]. A catalyst disk with a diameter of 7 mm and a thickness of c. 0.4–0.5 mm was placed on the measuring electrode in a vacuum chamber connected to a gas-supply system controlling the partial pressure of oxygen. The interaction of oxygen with the catalyst sample was studied in the temperature range from 623 to 723 K applying oxygen partial pressure between 2.5×10^{-4} and 5×10^{-3} Pa.

The character of the interaction in the metal oxide/oxygen system is essentially affected by the ionic transport in the oxide lattice. Depending on the sorption mechanism, two cases may be distinguished [13].

(1) The surface charge generated by chemisorption of oxygen is located at the surface as long as ionic transport in the lattice is quenched and sorption is limited to the adsorbed layer. For this case, increasing oxygen partial pressure results to an increase of CPD with time and then CPD reaches a constant value that corresponds to the chemisorption equilibrium. Information on the charge of surface oxygen species for a metal oxide/oxygen system might be derived according to Nowotny [13] and Barbaux et al. [14] from Eq. (1):

$$\mathrm{CPD} = \frac{kT}{ae} \ln p_{\mathrm{O}_2} + \mathrm{const} \qquad (1)$$

In this equation, a is the number of electrons transferred from the solid to the adsorbed oxygen species, i.e., changes in CPD caused by variations in oxygen partial pressure at constant temperature are directly related to the charge of surface oxygen species as it is shown below

$$a = 1 \qquad \mathrm{O}_2 + e \rightleftarrows \mathrm{O}_2^- \qquad (2)$$

$$a = 2 \qquad \mathrm{O}_2 + 2e \rightleftarrows 2\mathrm{O}^- \qquad (3)$$

$$a = 2 \qquad \mathrm{O}_2 + 2e \rightleftarrows \mathrm{O}_2^{2-} \qquad (4)$$

$$a = 4 \qquad \mathrm{O}_2 + 4e \rightleftarrows 2\mathrm{O}^{2-} \qquad (5)$$

(2) If ionic transport into the lattice takes place, the surface charge generated by oxygen adsorption decreases as a result of its migration in deeper layers of the oxide lattice. The charge decrease may be considered to be due either to an outward transport of anion vacancies (in the case of anion deficient oxides) or to diffusion of interstitial cations (in the case of oxides with Frenkel defects) or an inward transport of cation vacancies (in the case of cation deficient oxides). CPD increases initially with oxygen partial pressure increase and then decreases with time because of surface charge migration into the lattice.

2.4. TAP measurements

The TAP-2 reactor system has been described in detail elsewhere [15]. The catalyst (100 mg for Na_2O/CaO, 200 mg for Sm_2O_3 and $SmCa_5O_x$; $d_p = 250$–355 μm) was packed between two layers of quartz of the same particle size in the reactor. Before each experiment the catalyst was treated in a flow of O_2 (30 ml/min) at 873 K for c. 1 h. Then, the reactor was evacuated at 873 K to 10^{-4} Pa for 20 min. After the vacuum treatment, the temperature of the catalyst was set to the desired value between 673 and −873 K) and a mixture of $O_2/Ne = 1{:}1$ was pulsed over the catalysts.

2.5. TAP data treatment and fitting

The rate equations are solved by the so-called method of lines. The differential equations are first transformed into coupled ordinary differential equations by a spatial approximation and

then integrated by a numerical ordinary differential equation (ODE) solver. The kinetic parameters can be estimated by a non-linear regression analysis. More detail information on the subject was reported earlier [16,17]. The program used allowed a simple implementation of different models. Three models of oxygen interaction with catalyst surfaces described below were used in the present study.

2.6. Model 1: Langmuir-type adsorption

Assuming the Langmuir model for oxygen adsorption with the rate constants k_{ads} and k_{des},

$$O_2 + z \underset{k_{des}}{\overset{k_{ads}}{\rightleftarrows}} z{-}O_2 \tag{6}$$

the mass balance for the gas-phase and surface oxygen in the reactor can be written as

$$\frac{\partial C_{O_2}}{\partial t} = D_{eff}\frac{\partial^2 C_{O_2}}{\partial x^2} - C_{tot}\left(k_{ads}C_{O_2}(1-\Theta_{O_2}) - k_{des}\Theta_{O_2}\right) \tag{7}$$

$$\frac{\partial \Theta_{O_2}}{\partial t} = k_{ads}C_{O_2}(1-\Theta_{O_2}) - k_{des}\Theta_{O_2} \tag{8}$$

where $1 = \Theta_{O_2} + \Theta_z$, $\Theta_{O_2} = C_{z-O_2}/C_{tot}$, $\Theta_z = C_z/C_{tot}$ and D_{eff} is the effective Knudsen diffusion coefficient.

2.7. Model 2: One-stage reversible dissociative adsorption

For dissociative adsorption of gas-phase oxygen simultaneous oxygen adsorption and dissociation was assumed (Eq. (9)).

$$O_2 + 2z \underset{k_{des}}{\overset{k_{ads}}{\rightleftarrows}} 2z{-}O \tag{9}$$

For this model, the mass balance changes to

$$\frac{\partial C_{O_2}}{\partial t} = D_{eff}\frac{\partial^2 C_{O_2}}{\partial x^2} - C_{tot}^2\left(k_{ads}C_{O_2}(1-\Theta_O)^2 - k_{des}\Theta_O^2\right) \tag{10}$$

$$\frac{\partial \Theta_O}{\partial t} = 2C_{tot}\left(k_{ads}C_{O_2}(1-\Theta_O)^2 - k_{des}\Theta_O^2\right) \tag{11}$$

where $1 = \Theta_O + \Theta_z$, $\Theta_z = C_z/C_{tot}$, $\Theta_O = C_{z-O}/C_{tot}$ and D_{eff} is the effective Knudsen diffusion coefficient.

2.8. Model 3: Two-stage reversible dissociative adsorption

The reversible molecular adsorption occurs as the first step; the molecular precursor undergoes further dissociation with the participation of one more catalyst centre of the same nature. Model and mass balance can be written as follows:

$$O_2 + z \underset{k_{des}}{\overset{k_{ads}}{\rightleftarrows}} z{-}O_2 \tag{12}$$

$$z{-}O_2 + z \underset{k_{ass}}{\overset{k_{dis}}{\rightleftarrows}} 2\,z{-}O \tag{13}$$

$$\frac{\partial C_{O_2}}{\partial t} = D_{eff}\frac{\partial^2 C_{O_2}}{\partial x^2} - C_{tot}\left(k_{ads}C_{O_2}(1-\Theta_O - \Theta_{O_2}) - k_{des}\Theta_{O_2}\right) \tag{14}$$

$$\frac{\partial \Theta_{O_2}}{\partial t} = k_{ads}C_{O_2}(1-\Theta_{O_2}-\Theta_O) - k_{des}\Theta_{O_2} - C_{tot}\left(k_{dis}\Theta_{O_2}(1-\Theta_{O_2}-\Theta_O) - k_{ass}\Theta_O^2\right) \tag{15}$$

$$\frac{\partial \Theta_O}{\partial t} = 2C_{tot}\left(k_{dis}\Theta_{O_2}(1-\Theta_{O_2}-\Theta_O) - k_{ass}\Theta_O^2\right) \tag{16}$$

where $1 = \Theta_O + \Theta_{O_2} + \Theta_z$, $\Theta_{O_2} = C_{z-O_2}/C_{tot}$, $\Theta_z = C_z/C_{tot}$, $\Theta_O = C_{z-O}/C_{tot}$ and D_{eff} is the effective Knudsen diffusion coefficient.

3. Results and discussion

3.1. Catalytic performance

The catalytic results obtained on all the catalysts in the ODE are listed in Table 1. The contact times were varied to achieve similar degrees of ethane conversion. The main reaction product on all the catalysts was ethylene. Besides the formation of the undesired by-products CO and CO_2, small amounts of methane and C_3–C_4 hydrocarbons were formed. The selectivity towards ethylene were in the range between 53% and 78% depending on the type of catalyst. On a $Na_{0,00001}CaO_x$ catalyst containing sodium on the impurity level and thus approximating the pure CaO, an ethylene selectivity of 53.7% was obtained. With increasing sodium content C_2H_4 selectivity increased up to 78%. An improvement of selectivity was also achieved by doping of CaO with samaria.

For all catalysts studied, the selectivity of ethylene formation was affected by the ethane-to-oxygen ratio. Some of the dependencies are shown in Fig. 1. An increase in oxygen partial pressure results in increasing formation of total oxidation products. Although the participation of oxygen in the secondary gas-phase reactions cannot be completely ruled out the extension of surface oxidation on rising oxygen partial pressure is of high by probable. The latter can be due to increased formation of adsorbed oxygen species of non-selectively nature or/and to enhanced local concentration of these adsorbed species.

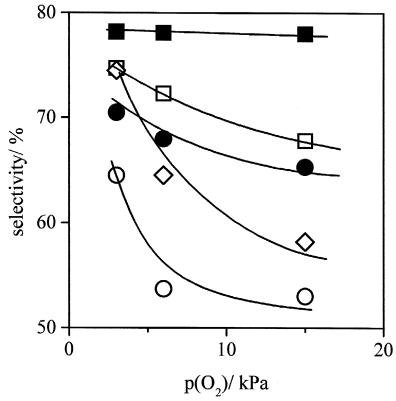

Fig. 1. Dependence of ethylene selectivity in ODE over the different catalysts vs. oxygen partial pressure: (○) $Na_{0,0001}CaO_x$; (□) $Na_{0,009}CaO_x$; (●) $Na_{0,012}CaO_x$; (■) $Na_{0,064}CaO_x$, (◇) $SmCa_5O_x$.

3.2. CPD

CPD measurements between an gold electrode and the catalysts were performed, to understand the differences between the catalysts for oxygen activation. The variations of CPD on changing oxygen partial pressure at different temperatures are shown in Fig. 2 for the $Na_{0,009}CaO_x$ catalyst. According to the theory of CPD (see above), its increase with increasing oxygen partial pressure is due to the formation of negatively charged oxygen species and their stabilisation on the catalyst surface. Applying Eq. (1) from which the information on the charge of surface oxygen species can be derived, the a values for the $Na_{0,009}CaO_x$ catalyst were estimated and amounted to 0.9 ± 0.1, 1.7 ± 0.2 and 1.7 ± 0.1 at 623, 673 and 723 K, respectively. The increasing values from 1 to

Table 1
Selectivity of formation of products in the oxidative dehydrogenation of ethane over different catalysts
Reaction condition: $p(C_2H_6) = 30$ kPa, $p(O_2) = 6$ kPa, total flow = 60 ml/min.

Catalyst	τ (g · s ml^{-1})	X (%)	C_2H_4	CO	CO_2	CH_4	C_3–C_4
$Na_{0,00001}CaO_x$	0.024	11.4	51.9	21.5	18.7	1.4	6.5
$Na_{0,009}CaO_x$	0.150	7.5	72.4	5.9	18.9	0.9	1.9
$Na_{0,012}CaO_x$	0.06	6.7	68.0	5.8	23.9	0.7	1.6
$Na_{0,064}CaO_x$	0.2	13.4	78.1	3.2	13.2	0.8	4.7
Sm_2O_3	0.025	17	61.4	11.3	16.7	1.1	9.5
$SmCa_5O_x$	0.02	10.7	64.5	11.8	17.0	2.2	4.5

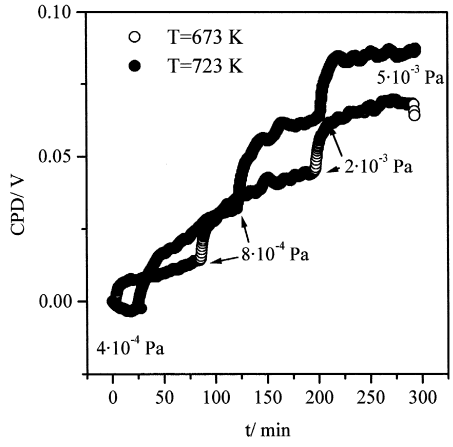

Fig. 2. CPD as a function of time (t) for $Na_{0,009}CaO_x$ at different temperatures after changes in oxygen partial pressure.

approximately 2 can be interpreted by the transformation of adsorbed molecular oxygen O_2^- formed at low to O^-/O_2^{2-} with increasing temperature. These data agree well with our earlier results on $Na_{0,012}CaO_x$, and $Na_{0,064}CaO_x$ catalysts [18]. We have also found a transformation of molecular oxygen species to atomic oxygen species with increasing temperature.

For Sm_2O_3, a successive enhancement of oxygen partial pressure at 673 and 723 K leads to a stepwise decrease of CPD as shown in Fig. 3. The decrease in CPD can be interpreted in terms of an ionic transport in the oxide lattice («CPD measurements»). After decreasing the oxygen partial pressure, CPD increases and reaches its initial value (Fig. 3). This means that a negative charge diffuses from the bulk to the surface followed by oxygen desorption. The assumption of oxygen incorporation into the deep oxide layers can be supported by the data of Cherrak et al. [19] who found that O^{2-} was the main oxygen species on Sm_2O_3 at temperatures higher that 360°C. It can be assumed that the temperature of our CPD measurements is high enough to enable the oxygen incorporation into deeper oxide layers. A high mobility of lattice oxygen in Sm_2O_3 agrees well with the results of Ekstrom and Lapszewicz [20] on oxygen isotopic exchange. They found that 100% of the lattice oxygen exchanged with gas-phase oxygen at high temperature.

Thus, the results of CPD studies show that an increase in temperature accelerates the transformation of molecular adsorbed oxygen into atomic oxygen species, the latter being incorporated into oxide lattice. The incorporation seems to take place between 673 and 723 K in the case of Sm_2O_3 while Na_2O/CaO requires higher temperatures to accomplish this step.

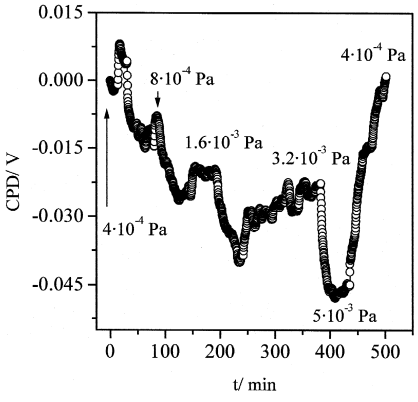

Fig. 3. CPD as a function of time (t) for Sm_2O_3 at 673 K after changes in oxygen partial pressure.

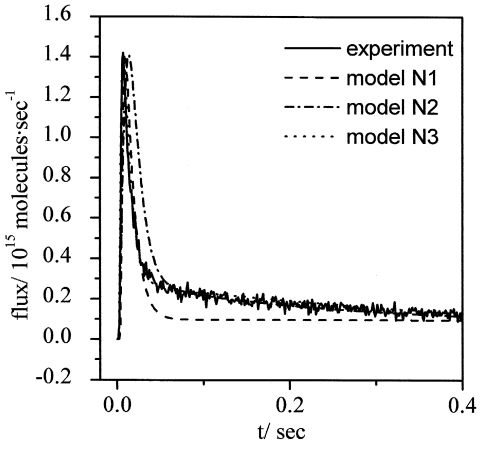

Fig. 4. Comparison among kinetic Models 1–3 for oxygen adsorption by the experimental response of oxygen over $Na_{0,00001}CaO_x$ at 873 K.

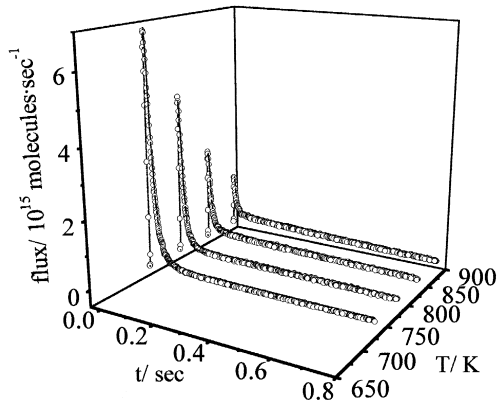

Fig. 5. Comparison between simulated (Model 3) and experimental (circles) responses of oxygen over $Na_{0,00001}CaO_x$ at different temperatures.

3.3. TAP responses fitting and relationship between catalyst composition and oxygen activation

To further elucidate the peculiarities of oxygen interaction with these catalysts, the modelling of TAP oxygen responses over different catalysts in the temperature range from 673 to 873 K was performed. The results of numerical fitting of the experimental data for oxygen adsorption are described. In Fig. 4, the experimental response of oxygen over $Na_{0.00001}CaO_x$ at 873 K is compared with the simulated responses obtained for the above mentioned models. Models 1 and 2 failed obviously to describe the transient behaviour. The best fitting of the experimental data was obtained by Model 3. This is valid for all the catalysts studied. It is necessary to note that a correlation between the three parameters (C_{tot}, k_{ads}, k_{dis}) was found, therefore, only the effective rate constants, which contain the total concentration of active sites ($k_{ads}^{eff} = C_{tot}k_{ads}$ and $k_{diss}^{eff} = C_{tot}k_{diss}$), were determined. A reference temperature was introduced to fit the experimental responses at different temperatures according to Eq. (17).

$$k_{T_i} = k_{T_{ref}} \exp\left(-\frac{E_a}{R}\left(\frac{1}{T_i} - \frac{1}{T_{ref}}\right)\right) \quad (17)$$

A good description of the transient data is obtained at each temperature (Fig. 5). This is valid for all the catalysts studied. Kinetic parameters obtained for different catalysts using Model 3 are summarised in Table 2. By analysing the kinetic data obtained, we can conclude that the ratio of k_{ads}/k_{dis} decreases in the following order:

$$Na_{0.00001}CaO_x > Na_{0.009}CaO_x > Na_{0.012}CaO_x > Na_{0.063}CaO_x > SmCa_5O_x > Sm_2O_3$$

The rate constants of association of atomic adsorbed oxygen were very low and have similar values for all Na_2O/CaO catalysts and Sm_2O_3 (Table 2). However, the rate constant of association of atomic oxygen on $SmCa_5O_x$ is to four to five orders of magnitude higher compared to all the catalysts studied (Table 2). One of the possible explanations of this later result might be the formation of peroxide ions in this

Table 2
Transient kinetic parameters for the elementary steps of oxygen interaction with different catalysts assuming Model 3

	k_{ads}^{eff}		k_{des}		k_{dis}^{eff}		k_{ass}	
	k_0^{eff}	E_a (kJ/mol)	k_0	E_a (kJ/mol)	k_0^{eff}	E_a (kJ/mol)	k_0	E_a (kJ/mol)
$Na_{0,00001}CaO_x$	9.1×10^{8}	89	6.6×10^{7}	116	1.5×10^{17}	249	2.3×10^{21}	420
$Na_{0,009}CaO_x$	5.9×10^{8}	94.5	5.8×10^{3}	31.6	1.6×10^{5}	61	9.2×10^{15}	311
$Na_{0,012}CaO_x$	2.1×10^{7}	70	6.5×10^{8}	106	3.9×10^{7}	94	1.9×10^{16}	292
$Na_{0,064}CaO_x$	8.6×10^{6}	80	1.6×10^{5}	67	8×10^{6}	88	6.5×10^{13}	253
Sm_2O_3	9.4×10^{7}	102	5.7×10^{24}	388	1×10^{25}	384	5.8×10^{19}	379
$SmCa_5O_x$	2.9×10^{21}	312	1.77×10^{21}	314	5.6×10^{21}	322	1.3×10^{21}	303

case. The ratio of k_{ads}/k_{dis} can indicate the ability of the catalyst for converting molecular adsorbed oxygen species to atomic adsorbed oxygen species. The results of TAP modelling are in agreement with those of CPD. From CPD results, it follows that for Sm_2O_3, O^{2-} are the main oxygen species at temperatures higher than 533 K [19] and these species can be incorporated into deeper oxide layers at temperatures higher as 673 K. For CaO-based catalysts, the formation of atomic species is possible only at temperatures higher as 673 K. Besides, we have earlier found that the incorporation of sodium cations into a CaO sublattice increases the anion conductivity and the amount of irreversibly adsorbed oxygen [18]. These effects were interpreted by formation of additional anion vacancies, which can catalyse the transformation of molecular adsorbed oxygen into atomic species.

Thus, from fitting the experimental oxygen responses, it is possible to conclude that the mechanism of oxygen interaction with the catalysts studied changes due to the incorporation both sodium and samarium cations into the calcium oxide lattice.

3.4. ODE and oxygen interaction

The catalysts studied showed marked difference in selectivity for the formation of ethylene in the selective dehydrogenation of ethane. To explain the dependence of the catalytic performances both on oxygen partial pressure and the catalyst composition, the mechanistic results on oxygen activation are discussed.

First, the analysis concerns Na_2O/CaO catalysts. As the catalytic results show, $Na_{0.00001}CaO_x$ has the lowest C_2-selectivity among all CaO-based catalysts and the ratio of k_{ads}/k_{dis} for oxygen activation is the highest for this catalyst. This means that $Na_{0.00001}CaO_x$ catalyst has the lowest ability to convert molecular adsorbed oxygen into atomic species. Earlier, from CPD and total conductivity measurements, we have concluded [18] that adsorbed oxygen species do not migrate into the oxide bulk, but stay and accumulate on the oxide surface. Using the kinetic parameters from the transient experiments, the surface coverages with molecular and atomic adsorbed oxygen species under steady-state oxygen conditions in the absence of ethane were simulated for different oxygen partial pressures. These data are then discussed to explain the catalytic performances of the catalysts in the ODE. Fig. 6 presents the selectivity of C_2 products formation over all Na_2O/CaO catalysts at different oxygen partial pressures vs. the ratio of Θ_O/Θ_{O_2} estimated at the same oxygen partial pressures as in the catalytic runs. From these results, it follows that the selectivity obtained grows with increasing the ratio of Θ_O/Θ_{O_2}. (Fig. 6). This means that a high selectivity of ethylene can be achieved by reducing the concentration of adsorbed molecular oxygen.

An incorporation of samarium oxide into the CaO lattice affects the catalytic performances of CaO. At low oxygen pressure, $SmCa_5O_x$ has the lowest CO_x selectivity among the catalysts studied except of $Na_{0.064}CaO_x$. With increasing oxygen partial pressure the selectivity of CO_x products growths very strongly. Promoting effect of samarium oxide on CaO is possible due to decreasing the ratio of k_{ads}/k_{dis} for oxygen activation. For this catalyst, in spite of the low

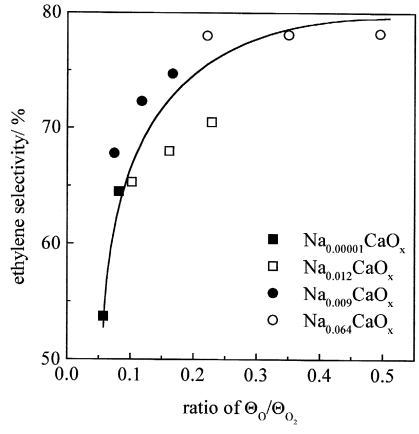

Fig. 6. Selectivity of ethylene formation over Na_2O/CaO catalysts in ODE versus steady-state ratio of Θ_O/Θ_{O_2} as simulated for different oxygen partial pressures in the absence of ethane.

ratio of k_{ads}/k_{dis} the ratio of Θ_O/Θ_{O_2} is very low as compared to Na_2O/CaO catalysts. This is due to a high value of k_{ass}. Under reaction conditions, the ratio of Θ_O/Θ_{O_2} will increase because of the reaction of atomic species with ethane or their diffusion into deep catalyst layers. The dependence of CO_x selectivity on oxygen partial pressure is well described, as in the case of Na_2O/CaO catalysts, by the reduced concentration of adsorbed molecular oxygen with decreasing oxygen partial pressure (Fig. 7).

The increase of CO_x selectivity with increasing concentration of adsorbed molecular oxygen species can be due to the fact that the polyatomic oxygen species promote especially C–C bond cleavage [4]. This reaction is probably the initial step of C_2 products combustion. The positive effect of the transformation of molecular oxygen in atomic oxygen surface species on selectivity was previously also found in our works for the OCM reaction [5,6,18,21]. Thus, the addition both of alkali dopant and samarium oxide into the CaO lattice influences the process of oxygen activation due to decreasing the ratio of k_{ads}/k_{dis}, which, in turn, results in reducing the coverage of the surface with molecular oxygen species and, hence, in high selectivity for C_2 products formation.

For Sm_2O_3, the highest selectivity of formation of C_3–C_4 hydrocarbons among the catalyst studied is typical (Table 1). Earlier [22], we have established that Sm_2O_3 is able to ignite C_2H_6–O_2 mixture at low temperature (450°C), with further reactions occurring most preferably in the gas phase. In this study, we had to reduce the amount of the catalysts to 10–20 mg to avoid ignition. In spite of reducing catalyst amount, we assume that the ignition of the mixture may influence our catalytic data. Work on elucidating this effect is in progress.

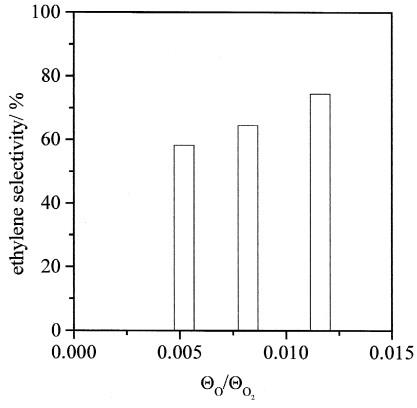

Fig. 7. Selectivity of ethylene formation over $SmCa_5O_x$ in ODE vs. steady-state ratio of Θ_O/Θ_{O_2} as simulated for different oxygen partial pressures in the absence of ethane.

4. Conclusions

Adsorption of gaseous oxygen studied by CPD measurements showed that the transformation of adsorbed molecular oxygen into atomic oxygen species above 673 K takes place, the type of this transformation depends on the catalyst composition. The results of CPD measurements were supported by modelling oxygen transient responses carried out in the TAP-2 reactor. From different models used for fitting the experimental data, a good fitting was only achieved when assuming the two-stage reversible dissociative adsorption via a molecular precursor. The kinetic constants simulated could be fitted with the Arrhenius law. It was found that the ratio of k_{ads}/k_{dis} determines the coverage of a catalyst surface with atomic vs. molecular oxygen and thus places a decisive role for the catalyst selectivity. A correlation between the ratio of Θ_O/Θ_{O_2} and selective oxidation of ethane was found. A decrease in the concentration of adsorbed molecular oxygen due to an increase of the rate of its dissociation improves the catalytic performances of Na_2O/CaO catalysts with increasing sodium concentration and by doping of CaO with Sm_2O_3.

5. Notation

C_{O_2} gas-phase oxygen concentration (mol · m^{-3} of gas phase)

C_z	concentration of free active catalyst centres ($mol \cdot m^{-3}$ of catalyst)
C_{z-O_2}	concentration of molecular adsorbed oxygen species ($mol \cdot m^{-3}$ of catalyst)
C_{z-O}	concentration of atomic adsorbed oxygen species ($mol \cdot m^{-3}$ of catalyst)
C_{tot}	total concentration of adsorption sites ($mol \cdot m^{-3}$ of catalyst)
D_{eff}	effective Knudsen diffusion coefficient ($m^2 \cdot s^{-1}$)
d_p	catalyst particle size (μm)
E_a	activation energy (kJ/mol)
k_{ads}	adsorption rate constant ($m^3 \cdot mol^{-1} \cdot s^{-1}$)
k_{des}	desorption rate constant (s^{-1})
k_{diss}	dissociation rate constant ($m^3 \cdot mol^{-1} \cdot s^{-1}$) — Model 3
k_{ass}	association rate constant ($m^3 \cdot mol^{-1} \cdot s^{-1}$) — Model 3
k_o	pre-exponential factor (s^{-1} and $m^3 \cdot mol^{-1} \cdot s^{-1}$ for reaction of first and second order, respectively)
Θ_{O_2}	fractional coverage of molecular adsorbed oxygen (dimensionless)
Θ_O	fractional coverage of atomic adsorbed oxygen (dimensionless)
Θ_z	fractional coverage of free adsorption sites (dimensionless)
t	time (s)
T	temperature (K)
x	reactor coordinate (m)

Acknowledgements

E.V. Kondratenko thanks Alexander von Humboldt Foundation for a postdoctoral fellowship to work at the Institut für Angewandte Chemie Berlin-Adlershof e.V. The work was supported by the German Federal Ministry for Education and Research (Contract No. 03C3-0120) and by the State of Berlin as well as by Fond der Chemischen Industrie.

References

[1] G.K. Boreskov, Catalytic activation of dioxygen, in: J. Andersen, M. Boudart (Eds.), Catalysis: Science and Technology, Springer, Berlin, 1982, p. 40.
[2] H.H. Kung, Adv. Catal. 40 (1994) 1.
[3] A. Belansky, J. Haber, Oxygen in Catalysis, Marcel Dekker, New York, 1996.
[4] M. Iwamoto, J.-H. Lunsford, J. Phys. Chem. 84 (1980) 3079.
[5] H. Borchert, M. Baerns, J. Catal. 168 (1997) 315.
[6] G. Gayko, D. Wolf, E.V. Kondratenko, M. Baerns, J. Catal. 178 (1998) 441.
[7] G.J. Hutchings, M.S. Scurrel, J.R. Woodhous, J. Chem. Soc.-Chem. Commun. 85 (1989) 2507.
[8] A.G. Anshits, V.G. Roguleva, E.V. Kondratenko, in: V. Cortes Corberan, S. Vic Belon (Eds.), Studies in Surface Science and Catalysis Vol. 82 Elsevier, Amsterdam, 1994, p. 337.
[9] E. Morales, J.H. Lunsford, J. Catal. 118 (1989) 255.
[10] H. Swaan, A. Toebes, K. Seshan, J.G. Van Ommen, J.R.H. Ross, Catal. Today 13 (1992) 629.
[11] L. Ji, J. Liu, Chem. Commun. (1996) 1203.
[12] O. Buyevskaya, M. Baerns, DGMK-Tagungsber. 9803 (1998) 139.
[13] L. Nowotny, J. Mater. Sci. Monogr. 15 (1982) 358.
[14] Y. Barbaux, J.P. Bonnelle, J.P. Beaufils, J. Chem. Res. M 556 (1979) .
[15] J.T. Gleaves, G.S. Yablonskii, P. Phanawadee, Y. Schuurman, Appl. Catal. 160 (1997) 55.
[16] M. Rothaemel, M. Baerns, Ind. Eng. Chem. Res. 35 (1996) 1556.
[17] M. Soick, D. Wolf, M. Baerns, Chem. Eng. Sci., submitted.
[18] E.V. Kondratenko, M. Baerns, D. Wolf, Catal. Lett. 58 (N4) (1999) 217.
[19] A. Cherrak, R. Hubaut, Y. Barbaux, J. Chem. Soc. Faraday Trans. 88 (1992) 3241.
[20] A. Ekstrom, J.A. Lapszewicz, J. Am. Chem. Soc. 110 (1988) 5226.
[21] A.G. Anshits, N.P. Kirik, V.G. Roguleva, A.N. Shigapov, G.E. Selyutin, Catal. Today 4 (1989) 399.
[22] O. Buyevskaya, M. Baerns, DGMK-Conference on ''Selective Oxidations in Pertochemistry, Hamburg'', 1998, p. 139.